Pseudodiffusive magnetotransport in graphene

Elsa Prada,[1] Pablo San-Jose,[1] Bernhard Wunsch,[2,3] and Francisco Guinea[3]
[1]*Institut für Theoretische Festköperphysik and DFG, Center for Functional Nanostructures (CFN), Universität Karlsruhe, D-76128 Karlsruhe, Germany*
[2]*Departamento de Física de Materiales, Universidad Complutense de Madrid, E-28040 Madrid, Spain*
[3]*Instituto de Ciencia de Materiales de Madrid, CSIC, Cantoblanco, E-28049 Madrid, Spain*
(Received 1 February 2007; published 27 March 2007)

Transport properties through wide and short ballistic graphene junctions are studied in the presence of arbitrary dopings and magnetic fields. No dependence on the magnetic field is observed at the Dirac point for any current cumulant, just as in a classical diffusive system, both in normal-graphene-normal and normal-graphene-superconductor junctions. This pseudodiffusive regime is, however, extremely fragile with respect to doping at finite fields. We identify the crossovers to a field-suppressed and a normal ballistic transport regime in the magnetic-field-doping parameter space, and provide a physical interpretation of the phase diagram. Remarkably, pseudodiffusive transport is recovered away from the Dirac point in resonance with Landau levels at high magnetic fields.

DOI: 10.1103/PhysRevB.75.113407 PACS number(s): 75.47.Jn, 72.80.Rj, 74.45.+c, 75.70.Ak

Low-energy excitations in a monolayer of carbon atoms arranged in a honeycomb lattice, known as a graphene sheet, have the remarkable peculiarity of being governed by the two dimensional massless Dirac equation, which is responsible for a variety of exotic transport properties as compared to ordinary metals. Particularly striking is that for clean, undoped graphene the density of states is zero, but not so the conductivity, which remains of the order of the quantum unit e^2/h.[1,2] Another intriguing fact is that a wide and short strip of undoped graphene exhibits "pseudodiffusive" transport properties in the absence of electron-electron interactions and impurity scattering.[3] By "pseudodiffusive" it is meant that transport properties are indistinguishable from those of a classical diffusive system. These include the full transport statistics (in particular, the Fano factor $F=1/3$ and the conductance $G \propto W/L$,[3] where W is the width and L is the length of the graphene strip), the critical current,[4] and I-V characteristics[5] in Josephson structures, as well as the relation of the normal-metal–superconductor conductance to the normal transmissions.[6] The same behavior can be expected in bilayer graphene.[7] In fact, all of the above similarities can be explained by noting that at the Dirac point (i.e., for undoped graphene) transport occurs entirely via evanescent modes with a transmission that is equal to the diffusive transport theory result (evaluated at $k_F l=1$, $l \equiv$ mean free path[24]) without quantum corrections,[3,6,8]

$$T_{k_y} = \frac{1}{\cosh^2 k_y L}. \tag{1}$$

Here, k_y is the transverse momentum of the channel. In diffusive systems, the above relation holds independently of an externally applied magnetic field in the limit of many channels (classical limit), for which any quantum weak localization correction is negligible.[8]

The question we raise here is as follows: Does the diffusive behavior of ballistic graphene persist in the presence of a magnetic field? We will show that for zero doping the equivalence is preserved for any magnetic field. Remarkably for a ballistic system, the applied magnetic field does not affect the transport statistics (for any current cumulant) at the Dirac point. For graphene with disorder, this has recently also been demonstrated at the conductivity level.[9–11] At sufficiently strong magnetic fields, an exponentially small chemical potential is enough to enter a field-suppressed transport regime. However, at resonance with the Landau levels (LLs) the pseudodiffusive behavior is recovered for all current cumulants. For even higher dopings, one observes a final crossover to the ballistic magnetotransport regime, since clean graphene then resembles a ballistic normal metal.

The magnetic field introduces a fundamental quantum-mechanical length scale known as the magnetic length $l_B = (\hbar/|e\vec{B}|)^{1/2}$. In the complete absence of scattering, localized LLs are well formed and ballistic transport is suppressed. The only contribution to transport in this regime comes from resonant tunneling exactly at Landau energies. In usual metals, this happens when the cyclotron diameter $2r_c = 2l_B^2 k_F$ is smaller than the relevant scattering length (set by system size, disorder, or temperature). If $2r_c$ is of the order of or larger than the scattering length, then delocalized states contribute to transport, leading to Shubnikov–de Haas oscillations and the quantum Hall effect. For wide and short ballistic strips, the relevant scattering scale is the strip length L, and scattering on lateral boundaries can be ignored. In graphene, the lowest LL lies precisely at the Dirac point. Besides, at this point $k_F=0$ and thus $r_c=0$ independent of the magnetic field. Therefore, in contrast to the normal-metal strip and to the high doping limit, at the Dirac point no delocalized bulk transport should take place for any magnetic field and resonant tunneling should be field independent.

To confirm this hand-waving picture, we analyze theoretically magnetotransport effects through normal-graphene-normal (N) and normal-graphene-superconductor (NS) wide ballistic junctions at arbitrary dopings and magnetic fields. From an experimental point of view, transport properties of lightly doped graphene in contact with superconductors are currently being investigated.[12] Moreover, the properties of

graphene in strong magnetic fields are also a subject of great interest,[13–15] in particular, in relation to weak (anti)localization.[16–20] Here, we consider a clean graphene sheet of width W (assumed to be the largest length scale in the system) in the y direction through which transport occurs in the x direction. For $x<-L/2$, it is covered by a normal contact, and for $x>L/2$, it is covered either by a superconducting contact or by a normal one. The central region is lightly doped, leading to a finite Fermi energy μ measured relative to the Dirac point, which can be varied by an external gate voltage. The contact regions are modeled as heavily doped graphene, with Fermi energy μ_c conveniently fixed to infinity with respect to both μ and the superconducting gap Δ. The boundary conditions in the y direction are irrelevant[3] for large aspect ratios $W/L \gg 1$. We choose periodic boundaries for simplicity. A constant external magnetic field B is applied perpendicular to the graphene sheet. We assume the electrodes to be magnetically shielded, e.g., by covering them with materials with high magnetic permeability. In the Landau gauge, we can write the vector potential as $\vec{A}=(0,Bx,0)$ for $|x|<L/2$, and constant in the contact regions. This gauge is convenient since the motions in the x and y directions are uncoupled and k_y remains a good quantum number. We neglect Zeeman splitting, so that the electron spin only enters as a degeneracy factor of 2 in the following calculation. Finally, we note that edge currents generally give a negligible contribution to transport in the $W \gg L$ limit.

We will compute the N and the NS (Andreev) inverse longitudinal resistivities, $\rho_{xx}^{-1}=G(L/W)$, expressed in terms of the conductances[3,6]

$$G_{\mathrm{N}}=\frac{4e^2}{h}\sum_{k_y} T_{k_y}, \quad G_{\mathrm{NS}}=\frac{8e^2}{h}\sum_{k_y}\frac{T_{k_y}^2}{(2-T_{k_y})^2}, \tag{2}$$

and the shot noise using corresponding expressions in terms of the transmission for normal conducting contacts T_{k_y}.[21] Note that the above expressions for the NS case are valid only if T_{k_y} is left-right symmetric, which is not in general true in the presence of a magnetic field. In our particular setup, it does indeed turn out to be symmetric. The transmission through the central region is obtained by imposing current conservation at the interfaces, which translates into continuity of the wave function. In the chosen gauge, the scattering problem is effectively one dimensional, the transverse mode profile $e^{ik_y y}$ being the same in all regions, so we will only discuss the x dependence of the wave functions from now on.

The contact region eigenstates at energy $\epsilon=\hbar v_F\sqrt{k_x^2+k_y^2}-\mu_c+\mu$ with respect to the central strip Dirac point are given by

$$\Psi^N_{k_x k_y s}(x)=\begin{pmatrix} s z_{\mathbf{k}}^{-s} \\ 1 \end{pmatrix} e^{ik_x x}. \tag{3}$$

The spinor lives in the space of the two triangular sublattices that conform the graphene hexagonal lattice, $s=\pm 1$ is the "valley" quantum number (for the degenerate K and K' points), and $z_{\mathbf{k}}\equiv\exp[i\arg(k_x+ik_y)]$, which tends to $z_{\mathbf{k}}\approx\mathrm{sgn}(k_x)$ when $\mu_c\to\infty$.

The spinor $\Psi^G_{\epsilon k_y s}(x)=[\phi^A_{\epsilon k_y s}(x),\phi^B_{\epsilon k_y s}(x)]^T$ for the central region is determined by the one-dimensional Dirac equation

$$\begin{pmatrix} 0 & -i\hat{a} \\ i\hat{a}^+ & 0 \end{pmatrix}\begin{pmatrix} \phi^A_{\epsilon k_y s}(x) \\ \phi^B_{\epsilon k_y s}(x) \end{pmatrix}=\lambda\sqrt{n_\epsilon}\begin{pmatrix} \phi^A_{\epsilon k_y s}(x) \\ \phi^B_{\epsilon k_y s}(x) \end{pmatrix}, \tag{4}$$

with $\hat{a}\equiv(\tilde{x}+\partial_{\tilde{x}})/\sqrt{2}$, $\hat{a}^+\equiv(\tilde{x}-\partial_{\tilde{x}})/\sqrt{2}$, $\tilde{x}\equiv x/l_B+k_y l_B$, $\lambda=\mathrm{sgn}\,\epsilon$, and $n_\epsilon=(l_B|\epsilon|/\hbar v_F)^2/2$. Canonical relations $[\hat{a},\hat{a}^+]=1$ are satisfied. The above equation corresponds to the K valley ($s=1$), while the $s=-1$ equation is obtained by swapping $\hat{a}$ and $\hat{a}^+$. Since the central region is bounded, no integrability condition must be met and the eigenspectrum of Eq. (4) is continuous. The usual LL solutions, which correspond to integer n_ϵ, are thus complemented by a larger family of divergent wave functions, typically localized around the interfaces $x=\pm L/2$, with arbitrary $n_\epsilon \geqslant 0$.[22] At the Dirac point ($n_\epsilon=0$), the components of the spinor are uncoupled, and the two eigenstates for $s=1$ are $\Psi^{G,1}_{0k_y 1}(x)=[0,\exp(-\tilde{x}^2/2)]^T$ and $\Psi^{G,2}_{0k_y 1}(x)=[\exp(+\tilde{x}^2/2),0]^T$. The $s=-1$ solution has interchanged spinor components. At finite energy ($n_\epsilon>0$), the solutions to Eq. (4) become

$$\Psi^{G,1(2)}_{\epsilon k_y 1}(x)=\begin{pmatrix} \lambda h^{e(o)}_{n_\epsilon-1}(\tilde{x}) \\ i h^{o(e)}_{n_\epsilon}(\tilde{x}) \end{pmatrix}, \quad \Psi^{G,1(2)}_{\epsilon k_y -1}(x)=\begin{pmatrix} \lambda h^{o(e)}_{n_\epsilon}(\tilde{x}) \\ i h^{e(o)}_{n_\epsilon-1}(\tilde{x}) \end{pmatrix}.$$

They have been expressed in terms of the even and odd (in $\tilde{x}$) solutions $h_n^{e,o}(\tilde{x})$ of the Klein-Gordon equation $a^+ a h_n^{e(o)}(\tilde{x})=n h_n^{e(o)}(\tilde{x})$ [the square of Eq. (4)], normalized so that $\hat{a}^+ h_n^{e(o)}=\sqrt{n+1}h_{n+1}^{o(e)}$, $\hat{a}h_n^{e(o)}=\sqrt{n}h_{n-1}^{o(e)}$. As a function of the confluent hypergeometric function ${}_1F_1(a,b,z)=1+\frac{a}{b}\frac{z}{1!}+\frac{a(a+1)}{b(b+1)}\frac{z^2}{2!}+\cdots$ and $S_n=\mathrm{sgn}\{\sin[\pi(n+1/2)/2]\}$, these are

$$h_n^e(\tilde{x})=\sqrt{\frac{(n-1)!!}{\sqrt{\pi}n!!}}S_{n+1}e^{-\tilde{x}^2/2}\ {}_1F_1\left(-\frac{n}{2},\frac{1}{2},\tilde{x}^2\right),$$

$$h_n^o(\tilde{x})=\sqrt{\frac{2n!!}{\sqrt{\pi}(n-1)!!}}S_n\tilde{x}e^{-\tilde{x}^2/2}\ {}_1F_1\left(-\frac{n-1}{2},\frac{3}{2},\tilde{x}^2\right).$$

Imposing continuity for each $\{k_y,\epsilon\}$ at the interfaces results in the following s-independent transmission probability:

$$T_{k_y,\epsilon}=|t_{k_y,\epsilon}|^2=\left|\frac{2g^N_{n_\epsilon}}{g^R_{n_\epsilon}-ig^I_{n_\epsilon}}\right|^2, \tag{5}$$

where

$$g_n^R=h_n^{e+}h_{n-1}^{e-}+h_{n-1}^{e+}h_n^{e-}-h_n^{o+}h_{n-1}^{o-}-h_{n-1}^{o+}h_n^{o-},$$

$$g_n^I=h_n^{o+}h_n^{e-}-h_n^{e+}h_n^{o-}+h_{n-1}^{e+}h_{n-1}^{o-}-h_{n-1}^{o+}h_{n-1}^{e-},$$

$$g_n^N=h_{n-1}^{e+}h_n^{e+}-h_{n-1}^{o+}h_n^{o+}=\frac{S_{2n+1/2}}{\sqrt{\pi n}}$$

are expressed in terms of the wave functions at the boundaries $h_n^{e(o)\pm}=h_n^{e(o)}\left(\pm\frac{L/2}{l_B}+k_y l_B\right)$. This gives the general trans-

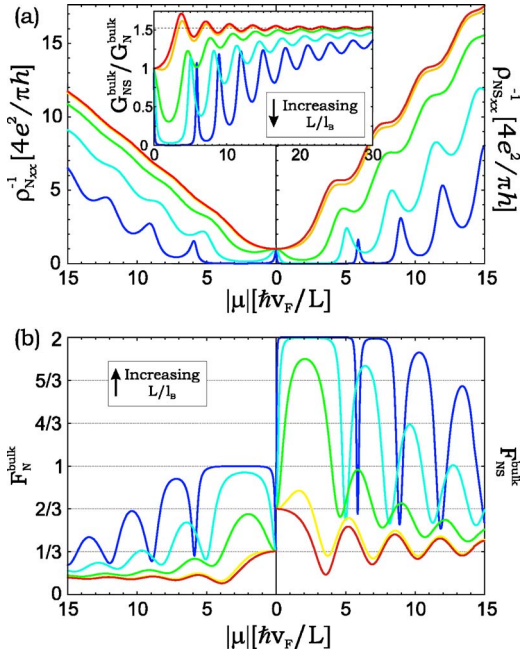

FIG. 1. (Color online) (a) Inverse longitudinal resistivity in units of $4e^2/\pi h$ and (b) bulk Fano factor for the N (left) and NS (right) junctions as a function of the (absolute value of the) Fermi energy (in units of $\hbar v_F/L$). Different curves correspond to different values of L/l_B (where $l_B \equiv \sqrt{\hbar/eB}$), which ranges from zero for red curve to 4 for the dark blue one in steps of 1. The same for the ratio $G_{\mathrm{NS}}^{\mathrm{bulk}}/G_{\mathrm{N}}^{\mathrm{bulk}}$ in the inset.

missions T_{k_y} for arbitrary doping and magnetic field. It reproduces previously known results at $B=0$ and nonzero doping[4] as well as Eq. (1) for $\mu=0$.

In Fig. 1(a), we plot ρ_{xx}^{-1} as a function of the Fermi energy for increasing values of the ratio $L/l_B \propto \sqrt{B}$. We recover the results obtained without magnetic field, namely, that σ_{N} and σ_{NS} [where $\sigma=\rho_{xx}^{-1}(B=0)$] tend to the known quantum-limited minimal conductivity value $4e^2/\pi h$ at zero doping, whereas for $|\mu|L/\hbar v_F \gg 1$ the slope of the asymptotes tends to 0.38π and 0.25π for the NS and N junctions, respectively.[6] Remarkably, as we increase B, all the ρ_{xx}^{-1} curves remain unchanged at the Dirac point $\mu=0$. The Dirac-point Fano factor in Fig. 1(b) is also unaffected by magnetic fields and takes the classical diffusive value (1/3 for the N and 2/3 for the NS junction). This happens for any current cumulant, since at $\mu=0$ the transmission given in Eq. (5) reduces to Eq. (1) independent of B.

However, for $\mu>0$ the resistivities and the Fano factors do depend on the magnetic field. In particular, for $2r_c<L$ (and above a certain critical value of L/l_B) transport can take place only at resonance with the LLs ($\mu L/\hbar v_F=\sqrt{2n}L/l_B$), while for other dopings ρ_{xx}^{-1} is suppressed as $e^{-(L/l_B)^2/2}$ for the N junction and as $e^{-(L/l_B)^2}$ for the NS one. The width of the resonances at the LL energies vanishes for $2r_c \ll L$, as we consider no disorder.[15] Remarkably, ρ_{xx}^{-1} at these resonances for large fields coincides with the one at the Dirac point $4e^2/\pi h$, a theoretical value that is usually associated strictly with zero doping and that is interestingly at odds with some experimental findings.[1] In fact, it can be analytically

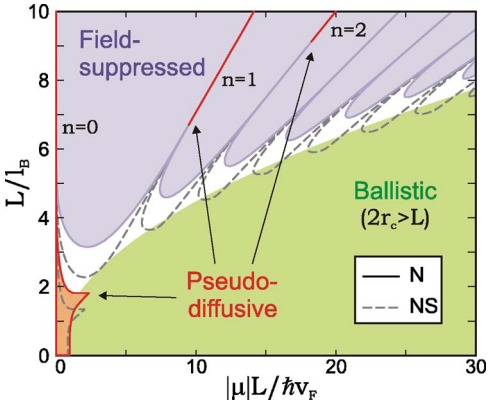

FIG. 2. (Color online) Phase diagram representing the crossovers from localized, pseudodiffusive, and ballistic transport regimes in the field-doping parameter plane. The solid (dashed) lines represent the boundaries for a N (NS) junction. LLs are labeled by n.

demonstrated that not only the conductance but the whole pseudodiffusive transport statistics is recovered at the resonances for high magnetic fields. Under this perspective, the field-independent resistivity at $\mu=0$ can be understood as due to resonant transport through the zeroth LL that remains pinned at the Dirac point. The field-suppressed regime is apparent for small but finite doping in Fig. 1(a), where ρ_{xx}^{-1} strongly decreases with increasing value of L/l_B. Correspondingly, the bulk Fano factor reaches the tunneling limit value (1 for the N and 2 for the NS junction) as transport gets suppressed [see Fig. 1(b)], in which limit the noise of the edge currents not considered here could be visible. Increasing the Fermi energy further, one enters the regime $2r_c>L$, where ρ_{xx}^{-1} is composed of two parts. The first part is linear in $\mu L/\hbar v_F$, in agreement with the scaling with L behavior of a ballistic conductor subject to a magnetic field (L-independent conductance). In particular, for sufficiently high dopings, all curves in Fig. 1(a) become parallel and tend to the same (average) slope as the zero-field conductivity. The second contribution to ρ_{xx}^{-1} is an oscillating part, which for $2r_c>L$ can no longer be explained by the resonance with LLs, since in that regime the effect of the boundaries is dominating the level structure in the central region. In fact, for $2r_c \gg L$ the oscillations become equally spaced and are explained rather by a Fabry-Pérot-type effect, connected to resonant tunneling through the structure.

In the inset of Fig. 1(a), the ratio $G_{\mathrm{NS}}^{\mathrm{bulk}}/G_{\mathrm{N}}^{\mathrm{bulk}}$ is plotted as a function of μ for the same values of L/l_B as in the main panel. At the Dirac point, the ratio goes to 1. At $\mu>0$, the suppressed magnetotransport manifests itself as a decaying $G_{\mathrm{NS}}^{\mathrm{bulk}}/G_{\mathrm{N}}^{\mathrm{bulk}} \propto e^{-(L/l_B)^2/2}$, until doping reaches the ballistic threshold and the ratio starts growing again, finally reaching its asymptotic value $0.38/0.25=1.52$. As explained in Ref. 6, this value is expected in normal ballistic systems with Fermi wavelength mismatch. Note again here that, for sufficiently suppressed G^{bulk}, the edge contribution[23] neglected here will dominate transport.

All the previous behaviors can be condensed in a quantitative way in the phase diagram shown in Fig. 2. It contains three regions corresponding to the three different transport

regimes, namely, pseudodiffusive (red), field suppressed (blue), and ballistic (green), in the L/l_B and $\mu L/\hbar v_F = k_F L$ parameter space. The corresponding crossover lines between regions are solid (dashed) for the N (NS) junction (note that the background colors correspond to the boundaries of the N case). The boundaries for the pseudodiffusive region have been calculated assuming a maximum deviation of ±10% with respect to the Dirac-point conductivity $4e^2/\pi h$. At low fields, the width of the pseudodiffusive window that brackets the Dirac point is roughly field independent, whereas for $L/l_B > 1.8$ for N (1.35 for NS) the window closes down as $\exp[-(L/l_B)^2/4]$. Physically, this means that at these higher fields the quasidiffusive transport regime is extremely fragile with respect to doping, and an exponentially fast crossover to the field-suppressed (localized) regime takes place. The boundaries of the latter (blue region) were set by a crossover criterion $\rho_{xx}^{-1} < 0.1(4e^2/\pi h)$. Its spiked shape is due to the peaked contributions to the field-suppressed ρ_{xx}^{-1} discussed in the analysis of Fig. 1, which are produced by resonant tunneling through LLs. When the magnetic field is increased, the positions of these peaks shift to higher dopings, converging on radial lines with slope $1/\sqrt{2n}$, while their width decreases exponentially. Above a certain value of L/l_B, the pseudodiffusive regime is recovered and the resonances are thus colored in red. The third region (green) is characterized by $\rho_{xx}^{-1} \propto L$ at fixed field and doping (which would correspond to radial lines in the phase diagram), and is therefore a ballistic transport regime. As expected from the arguments in the Introduction, the boundary of the field-suppressed region closely follows the ballistic threshold $2r_c = L$. Finally, intermediate regions (white) are characterized by strongly oscillating conductivities.

In conclusion, by computing the general transmission probabilities through short and wide graphene junctions, we have found that the transport properties at the Dirac point exactly match those of a classical diffusive system even in the presence of a magnetic field, which actually does not affect transport at all at zero doping. This behavior, which is associated with the existence of a zeroth LL pinned at the Dirac point, is, however, found to be exponentially fragile with respect to doping for high fields. By analyzing inverse longitudinal resistivity and higher current cumulants, we have identified and interpreted the three distinct regimes that appear at finite magnetic fields and dopings, corresponding to pseudo-diffusive, field-suppressed, and ballistic transport, and computed the phase diagram for the N and NS junctions in the relevant field-doping parameter space. Transport resonances at the LL energies are found in the field-suppressed regime, with ρ_{xx}^{-1} and all higher bulk current cumulants saturating to the pseudodiffusive Dirac-point values at high fields. The width of these resonances decreases exponentially with magnetic field, although broadening due to disorder in real samples is expected, thus facilitating experimental observation. The reappearance of pseudodiffusive transport at finite doping could shed light on the $1/\pi$ discrepancy between experiments and theoretical results for the conductivity at the Dirac point.

We thank G. Schön for support in promoting this collaboration. This work benefited from the financial support of the European Community under the Marie Curie Research Training Networks and the ESR program. F.G. acknowledges funding from MEC (Spain) through Grant No. FIS2005-05478-C02-01 and the European Union Contract No. 12881 (NEST).

[1] K. S. Novoselov *et al.*, Science **306**, 666 (2004).
[2] K. S. Novoselov *et al.*, Proc. Natl. Acad. Sci. U.S.A. **102**, 10451 (2005).
[3] J. Tworzydlo, B. Trauzettel, M. Titov, A. Rycerz, and C. W. J. Beenakker, Phys. Rev. Lett. **96**, 246802 (2006).
[4] M. Titov and C. W. J. Beenakker, Phys. Rev. B **74**, 041401(R) (2006).
[5] J. C. Cuevas and A. L. Yeyati, Phys. Rev. B **74**, 180501 (2006).
[6] A. R. Akhmerov and C. W. J. Beenakker, Phys. Rev. B **75**, 045426 (2007).
[7] I. Snyman and C. W. J. Beenakker, Phys. Rev. B **75**, 045322 (2007).
[8] C. W. J. Beenakker, Rev. Mod. Phys. **69**, 731 (1997).
[9] P. M. Ostrovsky, I. V. Gornyi, and A. D. Mirlin, Phys. Rev. B **74**, 235443 (2006).
[10] J. A. Vergés, F. Guinea, G. Chippe, and E. Louis, cond-mat/0610201 (unpublished).
[11] V. P. Gusynin and S. G. Sharapov, Phys. Rev. Lett. **95**, 146801 (2005).
[12] H. B. Heersche, P. Jarillo-Herrero, J. B. Oostinga, L. M. K. Vandersypen, and A. F. Morpurgo, Nature (London) **446**, 56 (2007).
[13] K. S. Novoselov *et al.*, Nature (London) **438**, 197 (2005).
[14] Y. B. Zhang *et al.*, Nature (London) **438**, 201 (2005).
[15] N. M. R. Peres, F. Guinea, and A. H. Castro Neto, Phys. Rev. B **73**, 125411 (2006).
[16] S. V. Morozov, K. S. Novoselov, M. I. Katsnelson, F. Schedin, L. A. Ponomarenko, D. Jiang, and A. K. Geim, Phys. Rev. Lett. **97**, 016801 (2006).
[17] A. F. Morpurgo and F. Guinea, Phys. Rev. Lett. **97**, 196804 (2006).
[18] E. McCann, K. Kechedzhi, V. I. Falko, H. Suzumara, T. Ando, and B. L. Altshnler, Phys. Rev. Lett. **97**, 146805 (2006).
[19] X. Wu, X. Li, Z. Song, C. Berger, and W. A. de Heer, cond-mat/0611339 (unpublished).
[20] K. Nomura and A. H. MacDonald, Phys. Rev. Lett. **98**, 076602 (2007).
[21] Y. M. Blanter and M. Büttiker, Phys. Rep. **336**, 2 (2000).
[22] A. D. Martino, L. Dell'Anna, and R. Egger, Phys. Rev. Lett. **98**, 066802 (2007).
[23] A. R. Akhmerov and C. W. J. Beenakker, cond-mat/0612698 (unpublished).
[24] It is noteworthy that the diffusive transport theory actually assumes weak disorder $k_F l \gg 1$. Hence, Eq. (1) is an extrapolation of the theory to a dirty metal limit.